ACADEMIC PRESS

Available online at www.sciencedirect.com

SCIENCE DIRECT

Journal of Solid State Chemistry 171 (2003) 317–323

JOURNAL OF SOLID STATE CHEMISTRY

http://elsevier.com/locate/jssc

Structure and magnetism in Pr_3ReO_7 and Nd_3ReO_7—materials with an ordered, defect fluorite structure

Robert Lam, Thomas Langet, and John E. Greedan*

Department of Chemistry, McMaster University, Brockhouse Institute for Materials Research, 1280 Main Street West, Hamilton, Ont., Canada L8S 4M1

Received 23 April 2002; received in revised form 15 July 2002; accepted 26 July 2002

Abstract

Nd_3ReO_7 and Pr_3ReO_7 were prepared by solid-state reaction involving Ln_2O_3, ReO_3 and ReO_2 in sealed quartz tubes and a carefully controlled thermal sequence. Attempts to prepare the corresponding compound with $Ln = La$ was unsuccessful with the same procedure. The crystal structures were refined from powder neutron diffraction data in space group *Cmcm*. The unit cell constants (Å) are $a = 10.941(1)$, $b = 7.4565(8)$ and $c = 7.5993(9)$ for $Ln = Pr$ and $a = 10.867(1)$, $b = 7.4594(7)$ and $c = 7.5740(8)$ for $Ln = Nd$. The structure type is a well-known variant of an ordered, defect fluorite. There are two *Ln* sites with pseudo-cubic 8-fold and pentagonal bipyramidal 7-fold coordination and Re^{5+} in an octahedral site. The Re–O octahedra share corners to form a zig-zag chain parallel to the *c*-axis. In both materials, Re^{5+} displays a local magnetic moment consistent with $S = 1$ and both show evidence for cooperative magnetic effects at low temperature. Pr_3ReO_7 appears to show spin glass order below about 10 K in the form of a zero-field-cooled–field-cooled divergence in the susceptibility, a hysteresis in the isothermal magnetization curves and the absence of magnetic Bragg peaks in the neutron powder pattern. For Nd_3ReO_7, by contrast, the bulk magnetic behavior is very complex but magnetic Bragg peaks appear in the neutron diffraction pattern below $T_c = 9\,K$, thus confirming long-range order. The magnetic Bragg peaks can be indexed with a wave vector, $\mathbf{k} = (000)$.

Keywords: Praseodymium (neodymium) rhenium (V) oxides; Ordered defect fluorites; Rietveld refinement from neutron diffraction; Spin glass; Magnetic long range order

1. Introduction

There exists a fairly extensive crystal chemistry based on the ordered, defect fluorite structure of stoichiometry Ln_3MO_7, where *Ln* is a rare earth and *M* is a pentavalent metal ion, usually from the 4*d* or 5*d* transition series, but the phase is also known for $M = Sb$ [1–7]. The relationship to the fluorite structure is as follows. The fluorite unit cell for oxides has the composition $M_4^{4+}O_8$. If the four tetravalent metal ions are replaced by three trivalent ions (*Ln*) and one pentavalent ion (*M*), one oxide vacancy is formed per fluorite cell. As well, due to the significant differences in radii between the Ln^{3+} and M^{5+} ions, cation ordering occurs on the metal sites and the oxide vacancy orders on the anion sites.

The end result is an orthorhombic supercell with dimensions $a \approx 2a_F$, $b \approx c \approx \sqrt{2}a_F$ and three distinct cation sites, one distorted cubic Ln^{3+} site, one distorted pentagonal bipyramidal Ln^{3+} site and one octahedral M^{5+} site. A striking feature of the structure is the presence of zig-zag chains of corner-sharing MO_6 octahedra along one of the orthorhombic axes (Fig. 1). These chains are well separated, the interchain distance > 6.6 Å, and thus, an element of quasi-one dimensionality is introduced to the *M*O sublattice. It has been pointed out recently that the *Ln* sublattice, taking the two sites together, is comprised of edge-sharing triangles and squares and is, thus, hospitable to geometric magnetic frustration [8]. Thus, one might expect interesting electronic properties when either Ln^{3+} or M^{5+} or both species have incomplete *d* or *f* shells. Several such systems have been investigated for various Ln^{3+} ions and M^{5+} = Mo, Ru, Ir and recently, Os [9–15]. A detailed summary of these results is beyond the

---

*Corresponding author. Fax: +905-522-2773.

E-mail address: greedan@mcmail.cis.mcmaster.ca (J.E. Greedan).

0022-4596/03/$ - see front matter © 2003 Elsevier Science (USA). All rights reserved.
doi:10.1016/S0022-4596(02)00210-4

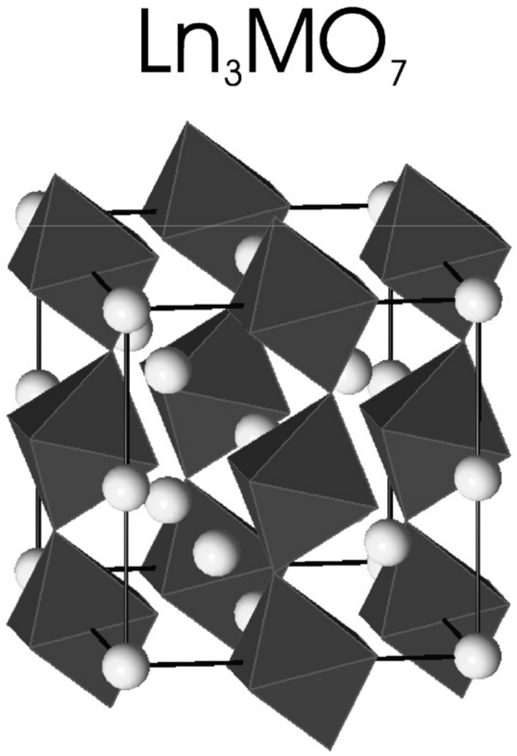

Fig. 1. The crystal structure of orthorhombic Ln_3MO_7 emphasizing the zig-zag chain of corner-sharing ReO_5 octahedra parallel to the *c*-axis. The spheres are the Ln^{3+} ions.

scope of this paper but in general, when M is non-magnetic, only paramagnetic behavior is seen to temperatures of ~4 K. The only known exceptions are for $M = Sb$ where long-range magnetic order is found for $Ln = Dy$ and Ho at 3 and 2 K, respectively [8]. When M is magnetic, evidence for long-range magnetic order is seen at temperatures up to ~50 K in some cases [11,12].

To date, there have been few reports of compounds where $M = Re$ ($5d^2$), to our knowledge; only the $Ln = Sm$ phase has been reported [7]. This material was found to be paramagnetic down to 4 K. In this report, efforts to expand the crystal chemistry of the $M = Re$ system and to characterize the products with respect to magnetic properties are described.

2. Experimental

2.1. Sample preparation

The following solid-state reaction was used to attempt the preparation of phases for $Ln = La$, Pr and Nd:

$$\tfrac{3}{2}Ln_2O_3 + \tfrac{1}{2}ReO_3 + \tfrac{1}{2}ReO_2 \rightarrow Ln_3ReO_7.$$

La_2O_3 and Nd_2O_3 (Rhone-Poulenc, 99.99%) were prefired at 1000°C for ~8 h before use. Pr_2O_3 was prepared by firing Pr_6O_{11} (Rhone-Poulenc, 99.99%) in an H_2 stream at 900°C for 12 h. The powders were mixed and ground using an agate mortar and pestle. The Re oxides (rhenium alloys) were used as obtained. Pressed pellets were placed in a platinum crucible, which was then contained in an evacuated, sealed quartz ampoule. The ampoule was loaded into a tube furnace and protected by a ceramic tube. The following heating schedule was used:

(1) R.T. → 300°C (6 h) (hold for 12 h)
(2) 300°C → 650°C (12 h) (hold for 24 h)
(3) 650°C → 1000°C (12 h) (hold for 24 h, furnace cool to room temp.)

The gradual temperature increase was necessary to prevent explosion of the ampoule due to dissociation of the Re oxides. Regrinding and refiring steps were often needed to produce single-phase materials. About 3 g of material, in the form of a black powder, was produced for each compound. The above procedure was successful only for Pr and Nd; the La phase could not be prepared. The major product in this case was La_2ReO_5 and a mixture of unidentified phases.

2.2. X-ray diffraction

The synthesized powders were checked for phase purity by X-ray powder diffraction using a Bruker D8 diffractometer with Cu$K\alpha$ radiation and an exit beam graphite monochromator. Rietveld refinement was carried out to confirm the phase purity and determine the unit cell constants using the FULLPROF code in the WINPLOT format [16].

2.3. Magnetic measurements

Powdered samples of ~50–100 mg were placed in a gelatin capsule holder and weighed accurately prior to data collection. Zero-field-cooled (ZFC) and field-cooled (FC) susceptibility data were collected on a quantum design MPMS SQUID magnetometer between 2 and 350 K in a range of applied fields. Data to 600 K were obtained with an "oven" insert and the sample was contained in a small diameter quartz tube. A small diamagnetic correction, -1.7×10^{-4} emu/mol, was applied to the data. Isothermal field sweeps were also carried out at selected temperatures over the range ~0.0–5.5 T. In a few cases, full hysteresis loops were measured.

2.4. Neutron diffraction

Data were collected at the C2 diffractometer operated by the Neutron Program for Materials Research (National Research Council of Canada) at the Chalk River Nuclear Laboratories, Chalk River, Ontario.

Different neutron wavelengths were used for the collection of data for crystal structure refinements, 1.3278(2) Å, and for magnetic peak searches, 2.3626(2) Å. The samples were contained in vanadium cans sealed with indium gaskets under an atmosphere of He exchange gas. The sample cans were loaded into an Oxford Instruments Orange cryostat and the temperature was controlled to within ±0.1 K over the range 2–295 K. Refinements were also done with FULLPROF in the WINPLOT format [16].

3. Results and discussion

3.1. Structural characterization

Both samples, Pr_3ReO_7 and Nd_3ReO_7, appeared to be single phase from the D8 data. The refined cell constants (Å) were $a = 10.964(1)$, $b = 7.4712(9)$ and $c = 7.6163(8)$ for the Pr phase and $a = 10.8478(6)$, $b = 7.4463(4)$ and $c = 7.5602(4)$ for the Nd material. For structural refinement, the neutron powder data were

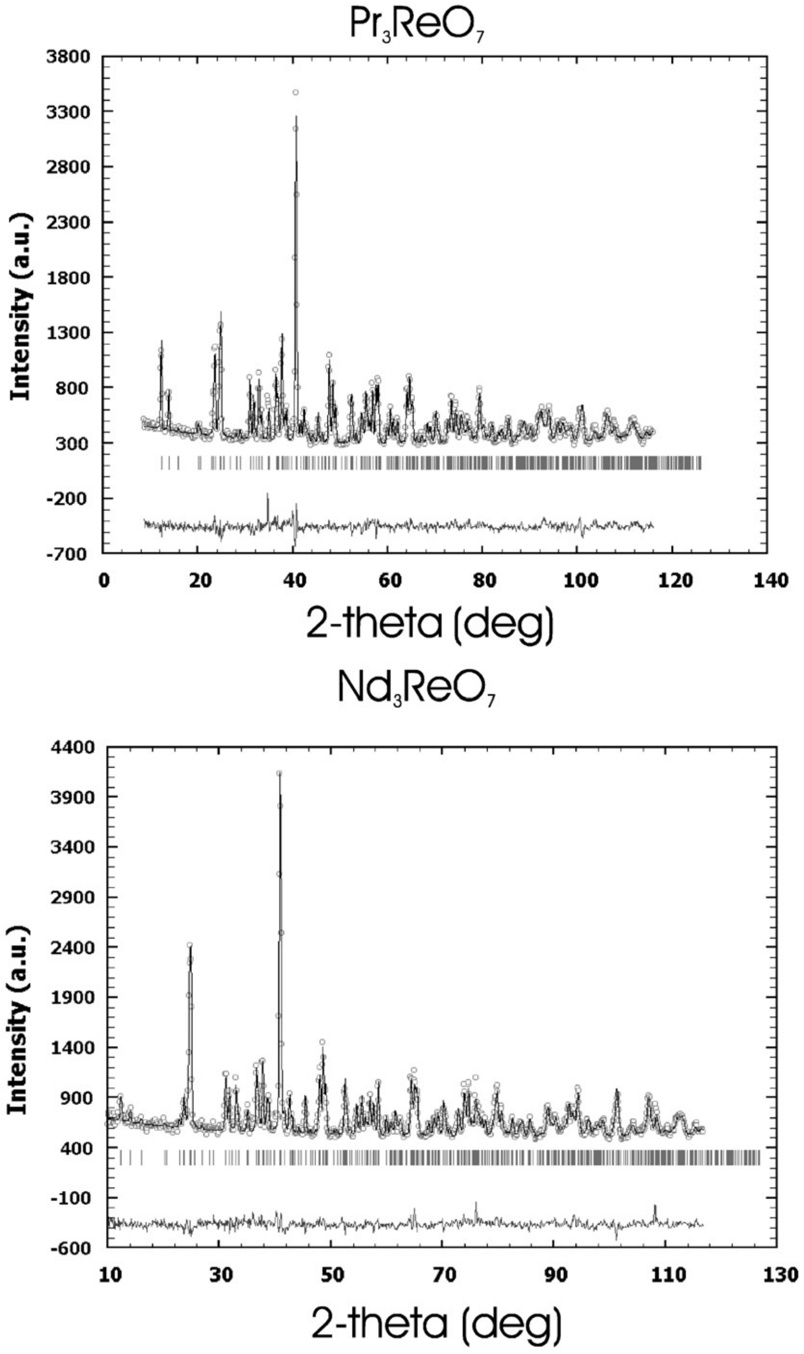

Fig. 2. Profile refinement of powder neutron diffraction data for Pr_3ReO_7 and Nd_3ReO_7. The data are the open circles, the fit is shown by the solid line, the vertical tick marks locate the Bragg peak positions and the difference plot is at the bottom.

Table 1
Rietveld refinement results for Ln_3ReO_7 (Ln = Pr, Nd; *Cmcm*)

	Pr				Nd			
a (Å)	10.941(1)				10.867(1)			
b (Å)	7.4566(8)				7.4594(7)			
c (Å)	7.5993(9)				7.5740(8)			
	x	y	z	B (Å^2)	x	y	z	B (Å^2)
*Ln*1	0.2730(6)	0.3047(9)	0.25	0.23(12)	0.2733(5)	0.3020(6)	0.25	0.20(14)
*Ln*2	0.0	0.5	0.0	0.62(19)	0.0	0.5	0.0	0.25(13)
Re	0.0	0.0	0.0	0.42(20)	0.0	0.0	0.0	0.10(15)
O1	0.5	0.429(1)	0.25	0.49(16)	0.5	0.428(1)	0.25	0.72(19)
O2	0.1243(4)	0.1832(5)	0.0384(5)	0.63(8)	0.1254(5)	0.1846(7)	0.0366(7)	0.70(10)
O3	0.3676(6)	0.0281(8)	0.25	0.52(12)	0.3674(7)	0.0280(9)	0.25	0.61(20)
R_{wp}		0.0646				0.0486		
χ^2		1.95				1.65		
R_B		0.0822				0.0917		

Table 2
Selected interatomic distances (Å) and angles (deg) in Ln_3MO_7 (Ln = Pr, Nd)

	Pr	Nd
*Ln*1–O1	2.6495(74)	2.6417(64)
*Ln*1–O2 × 2	2.4608(66)	2.4418(65)
*Ln*1–O2 × 2	2.4646(52)	2.4389(57)
*Ln*1–O3	2.3075(89)	2.2918(93)
*Ln*1–O3	2.2675(91)	2.2680(95)
*Ln*2–O2 × 4	2.7415(40)	2.7327(52)
*Ln*2–O3 × 4	2.3983(39)	2.3888(50)
Re–O1 × 2	1.9731(21)	1.9679(28)
Re–O2 × 4	1.9492(40)	1.9534(52)
Re–O1–Re	148.67(9)	148.40(12)

used and the results are shown in Fig. 2 and tabulated in Tables 1 and 2. The refinement was carried out in *Cmcm*. The positional parameters are in excellent agreement with those obtained from single crystal data on Sm_3ReO_7 [7]. From the bond distances of Table 2, it is clear that *Ln*(1) is 7-fold coordinated by O and *Ln*(2) is 8-fold coordinated. The Re–O distances are also consistent with the results for the Ln = Sm phase with an average distance of 1.958 Å for both Pr and Nd materials compared to 1.945 Å for Sm. The sum of the ionic radii for Re^{5+}–O is 1.96 Å assuming a mean coordination number for O^{2-} of 4 [17]. The Re–O–Re angles along the corner-sharing chain of octahedra are in the same range as found for other Ln_3MO_7 phases, 148.67(9)° and 148.4(1)°, respectively, for Ln = Pr and Nd.

The apparent instability of the Ln = La phase in this series is perhaps surprising on the basis of simple radius ratio considerations. The radius ratio, La/Re, is 1.75 (assuming a weighted average of VII and VIII coordinations for La) which lies between that for M = Mo (1.68) and M = Os (1.76) or M = Ru (1.79) for each of which the La_3MO_7 phase is found. The Ln = La phase is also not reported for M = Ir (1.77).

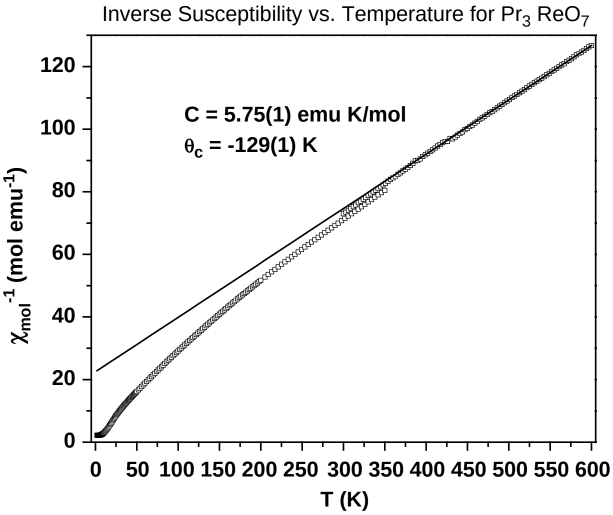

Fig. 3. Curie–Weiss fit to the inverse susceptibility for Pr_3ReO_7.

3.2. Magnetic properties

3.2.1. Pr_3ReO_7

Data taken up to 600 K show that the Curie–Weiss law is found, eventually, but only near 300 K and above (Fig. 3). The derived fitting constants are $C = 5.75(1)$ emu K/mol and $\theta_c = -129(1)$ K. First, the Curie constant can be compared with that for isostructural Pr_3TaO_7 for which Ta^{5+} is diamagnetic, $C = 4.63(3)$ emu K/mol, which should provide a reasonable estimate of the Pr^{3+} contribution [11]. This gives a value of $C(Re^{5+}) = 1.12(3)$ emu K/mol, which is close to the expected spin-only value of 1.00 emu K/mol for a d^2 configuration. Given the assumptions involved, this is in reasonable agreement and the indication is that a local moment appropriate to the $S = 1$ state ion can be assigned to

Re^{5+} in this material. The observed θ_c is more negative than that for Pr_3TaO_7, which is -54 K. In this material, the exchange contribution to θ_c is expected to be small, so the observed value is mainly the crystal field component. Thus, there is evidence for a relatively large, negative contribution from Re–Re and Re–Pr exchange.

This behavior contrasts sharply with that for Pr_3RuO_7 where a positive θ_c was taken as evidence for a ferromagnetic Pr–Ru interaction [11]. Fig. 4 shows evidence for a ZFC–FC divergence beginning below ~10 K and a broad maximum in the ZFC data near 3 K. Such behavior is often seen in spin glasses. In Fig. 5 isothermal magnetization loops indicate the onset of hysteresis again below 10 K, another signature of a spin glass-like state.

3.2.2. *Nd_3ReO_7*

From Fig. 6 it is clear that Curie–Weiss behavior is obtained above ~300 K with fitting parameters $C = 5.89(6)$ emu K/mol and $\theta_c = -99(6)$ K. Again, these values should be compared with the corresponding ones for the Ta analog which are $C_m = 4.95(5)$ emu K/mol and $\theta_c = -67(4)$ K [18]. Thus, it is possible to assign a $C(Re^{5+}) = 0.94(11)$ emu K/mol, appropriate to a $S = 1$ local moment. As with Pr_3ReO_7, the more negative Weiss temperature relative to Nd_3TaO_7 indicates predominantly antiferromagnetic Re–Re and Re–Nd exchange. The low-temperature susceptibility shows complex behavior, Fig. 7, with a ZFC–FC divergence near ~17 K and prominent maxima at 12 K (ZFC), 8 K (FC) and 3 K (FC). Fig. 8 displays

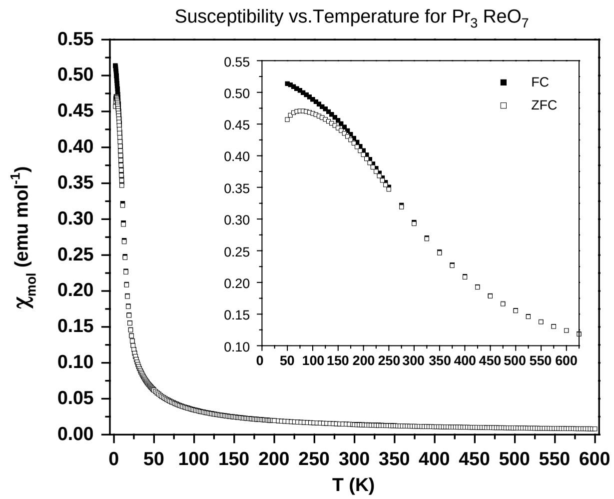

Fig. 4. Low-temperature ZFC and FC susceptibility for Pr_3ReO_7 showing the divergence below ~10 K and a weak maximum at 3 K (ZFC).

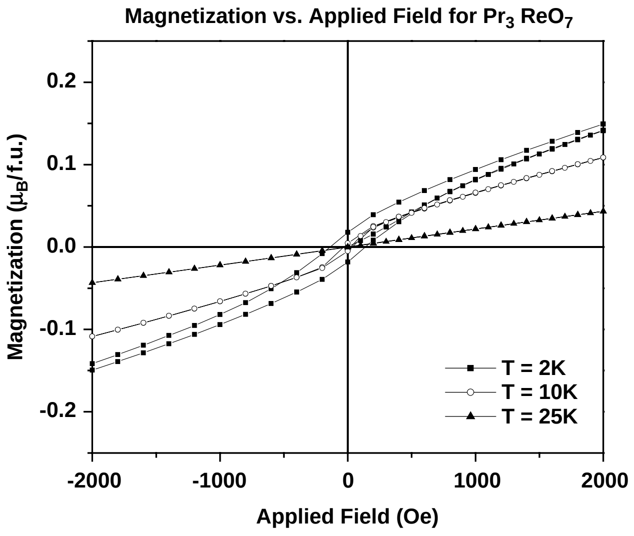

Fig. 5. Isothermal magnetization loops at selected temperatures for Pr_3ReO_7. Hysteresis is seen below 10 K.

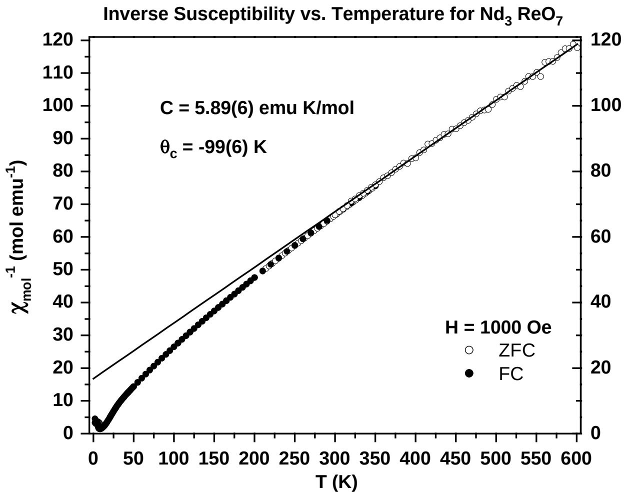

Fig. 6. Curie–Weiss fit to the inverse susceptibility for Nd_3ReO_7.

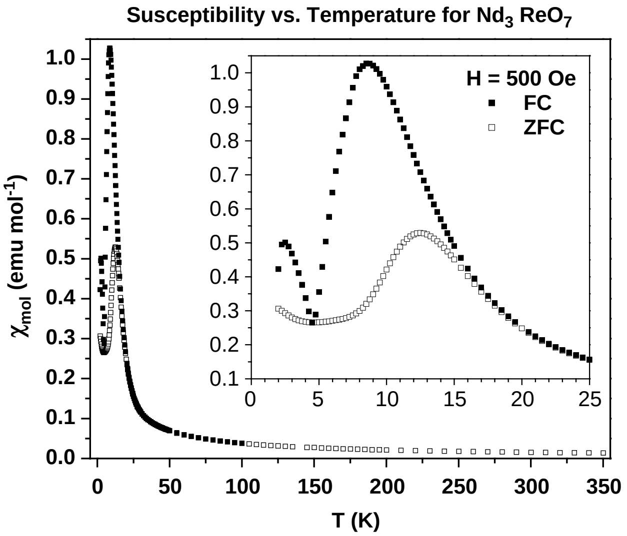

Fig. 7. Low-temperature ZFC and FC susceptibility for Nd_3ReO_7 showing both the divergence and the maxima in the ZFC and FC curves.

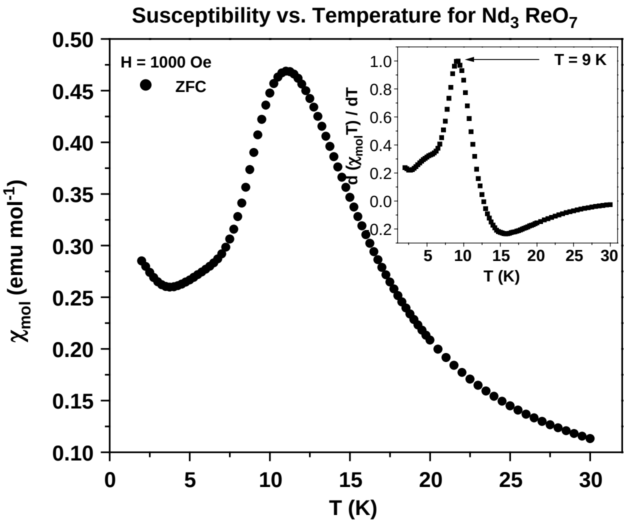

Fig. 8. The ZFC susceptibility for Nd_3ReO_7 at an applied field of 500 Oe. The inset shows the Fisher heat capacity [19] which indicates a $T_c = 9$ K.

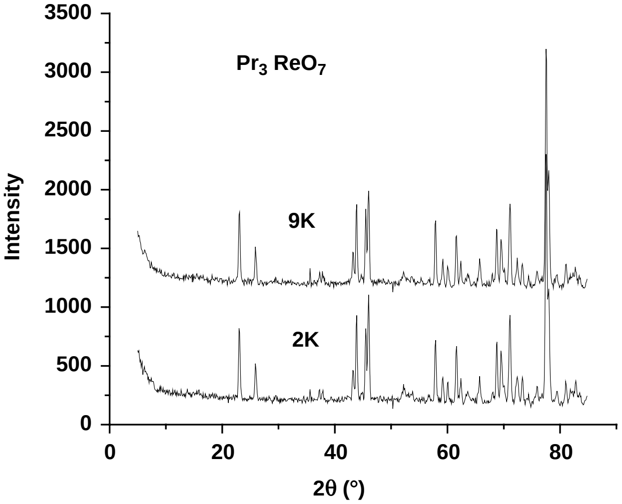

Fig. 9. Neutron diffraction patterns for Pr_3ReO_7 at 9 and 2 K. No new reflections appear at low temperatures.

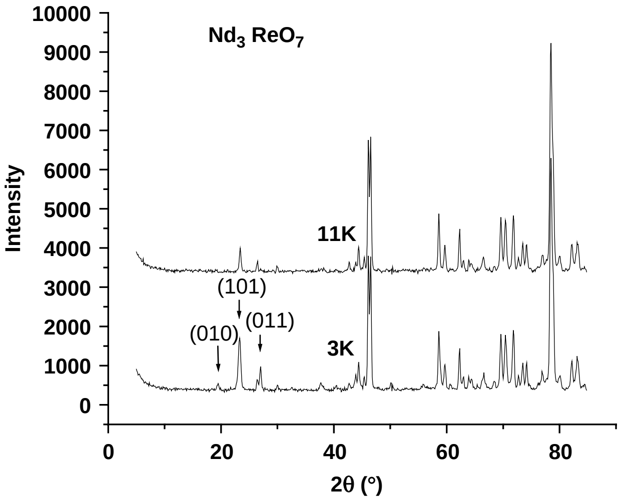

Fig. 10. Neutron diffraction patterns for Nd_3ReO_7 at 11 and 3 K. New reflections appearing at low temperatures are indicated and indexed on the chemical cell.

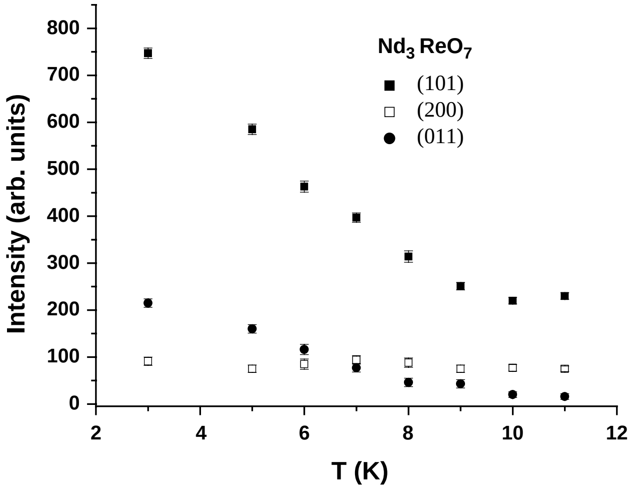

Fig. 11. The temperature dependence of the magnetic reflections (101) and (011) for Nd_3ReO_7 compared with the nuclear reflection (200). (101) also contains a nuclear component. A T_c below 10 K is indicated.

the temperature dependence of the Fisher heat capacity function, $d\chi T/dT$, and the sharp maximum at 9 K is indicative of long-range ordering [19].

3.3. Magnetic neutron diffraction

Evidence for magnetic order was sought using neutron diffraction. For Pr_3ReO_7 data were taken at temperatures above and below the ZFC–FC divergence temperature of ~10 K. No new reflections were observed down to 2 K, Fig. 9, which indicates the absence of long-range magnetic order at least to this temperature. This is consistent with the spin glass-like behavior seen in the bulk susceptibility. The situation for Nd_3ReO_7 is quite different (Fig. 10). Three reflections which can be indexed on the chemical cell, (010), (101) and (011), are strongly enhanced at 3 K relative to 13 K. The temperature dependence of the two strongest reflections, (101) and (011), Fig. 11, indicates a $T_c \sim 9$ K which is consistent with the result from the Fisher heat capacity analysis, Fig. 8, and is strong evidence for long-range magnetic order in this compound.

Work is ongoing to solve the magnetic structure.

4. Summary and conclusions

Two new members of the Ln_3ReO_7 series of materials with ordered, defect fluorite structures, Ln = Pr and Nd have been prepared and characterized with respect to crystal structure and magnetic properties. Both appear to crystallize in *Cmcm*. Efforts to prepare the Ln = La member, using the same synthetic approach was not successful. On the basis of a simple radius ratio criterion, this compound is expected to be stable in this structure type.

As might be expected for two materials with such close structural and chemical similarities, Pr_3ReO_7 and Nd_3ReO_7 exhibit similar magnetic properties at least at high temperatures. Both show Curie–Weiss paramagnetism near and above 300 K and there is strong evidence for a local moment on Re^{5+} appropriate to $S = 1$, consistent with the $5d^2$ (nominally t_{2g}^2) configuration, and net antiferromagnetic exchange. Nonetheless, their magnetic properties are remarkably different at low temperatures. The ground state of the Pr-phase appears to be spin glass-like down to 3 K from both bulk d.c. susceptibility and neutron diffraction. In contrast, the ground state for Nd_3ReO_7 involves long magnetic order with $T_c = 9\,K$. The properties of Pr_3ReO_7 present a remarkable contrast as well to Pr_3RuO_7 which shows evidence for short-range ferromagnetic correlations and a long-range ordered ground state with $T_c = 50\,K$. Considering that the principle electronic difference between these two materials is one extra electron in the t_{2g} levels for the Ru phase (Ru^{5+} is t_{2g}^3), the extent of the differences in magnetism is remarkable and not understood in any simple way, except to note that, clearly, Pr–Re and Pr–Ru exchange interactions are quite different. Studies are ongoing to solve the magnetic structure for Nd_3ReO_7 and to further characterize both materials using heat capacity and a.c. susceptibility.

Acknowledgments

We thank Dr. J.S. Gardner of the Neutron Program for Materials Research for assistance with the neutron diffraction studies. This work was supported by the Natural Sciences and Engineering Research Council through a Research Grant to J.E.G.

References

[1] D.K. Nath, Inorg. Chem. 9 (1970) 2714.
[2] J.G. Allpress, H.J. Rossell, J. Solid State Chem. 27 (1979) 105.
[3] H.J. Rossell, J. Solid State Chem. 27 (1979) 115.
[4] F.P.F. van Berkel, D.J.W. Ijdo, Mater. Res. Bull. 21 (1986) 1103.
[5] W.A. Groen, F.P.F. van Berkel, D.J.W. Ijdo, Acta Crystallogr. C 43 (1986) 2262.
[6] H. Prevost-Czeskleba, J. Less, Comm. Met. 127 (1987) 117.
[7] G. Wltschek, H. Paulus, I. Svoboda, H. Ehrenberg, H. Fuess, J. Solid State Chem. 125 (1996) 1.
[8] T. Fennell, S.T. Bramwell, M.A. Green, Can. J. Phys. 79 (2001) 1415.
[9] J.E. Greedan, N.P. Raju, A. Wegner, P. Gougeon, J. Padiou, J. Solid State Chem. 129 (1997) 320.
[10] P. Kalifah, R.W. Erwin, J.W. Lynn, Q. Huang, B. Batlogg, R.J. Cava, Phys. Rev. B 60 (1999) 9573.
[11] F. Wiss, N.P. Raju, A.S. Wills, J.E. Greedan, Intern. J. Inorg. Mater. 2 (2000) 53.
[12] D. Harada, Y. Hinatsu, J. Solid State Chem. 158 (2001) 245;
D. Harada, Y. Hinatsu, J. Phys.: Condens. Matter 13 (2001) 10825;
D. Harada, Y. Hinatsu, J. Solid State Chem. 164 (2002) 163.
[13] B.P. Bontchev, A.J. Jacobson, M.M. Gospodinov, V. Skumryev, V.N. Popov, B. Lorenz, R.L. Meng, A.P. Litvinchuk, M.N. Iliev, Phys. Rev. B 62 (2000) 12235.
[14] J.F. Vente, D.J.W. Ijdo, Mater. Res. Bull. 26 (1991) 1255.
[15] R. Lam, F. Wiss, J.E. Greedan, J. Solid State Chem. 167 (2002) 182.
[16] T. Roisnel, J. Rodriguez-Carvajal, Mater. Sci. Forum 378–381 (2001) 118.
[17] R.D. Shannon, Acta Crystallogr. A 32 (1976) 751.
[18] F. Wiss, J.E. Greedan, unpublished result.
[19] M.E. Fisher, Philos. Mag. 17 (1962) 1731.